



NLC Collimation Study Update: Performance with Tail Folding Octupoles

**A. Drozhdin¹, L. Keller², T. Markiewicz²,
T. Maruyama², N. Mokhov¹, T. Raubenheimer²,
A. Seryi², P. Tenenbaum², M. Woodley²,**

¹Fermi National Accelerator Laboratory
Batavia, IL

²Stanford Linear Accelerator Center
Menlo Park, CA

Abstract: This note describes an update to the study of linear collider collimation system performance performed by the collimation task force and presented in [1, 2, 3]. In particular, the performance of the NLC collimation system with the addition of “tail-folding” octupoles is described. These octupoles allow the betatron collimation gaps to be opened by more than a factor of three. We present the optimized gap settings, the location of additional photon masks, and the resulting synchrotron-radiation collimation efficiency. The studies confirm that the tail-folding octupoles are efficient, give additional flexibility, and enhance the collimation system performance.

NLC Collimation Study Update: Performance with Tail Folding Octupoles

A. Drozhdin¹, L. Keller², T. Markiewicz²,
T. Maruyama², N. Mokhov¹, T. Raubenheimer²,
A. Seryi², P. Tenenbaum², M. Woodley²,

¹Fermilab, Batavia, IL

²SLAC, Stanford, CA

Abstract

This note describes an update to the study of linear collider collimation system performance performed by the collimation task force and presented in [1, 2, 3]. In particular, the performance of the NLC collimation system with the addition of “tail-folding” octupoles is described. These octupoles allow the betatron collimation gaps to be opened by more than a factor of three. We present the optimized gap settings, the location of additional photon masks, and the resulting synchrotron-radiation collimation efficiency. The studies confirm that the tail-folding octupoles are efficient, give additional flexibility, and enhance the collimation system performance.

1 Introduction

The performance of the collimation systems designed for JLC/NLC, CLIC and TESLA linear colliders was compared by the TRC collimation task force and presented in [1, 2, 3]. These studies showed that the NLC collimation system had the best performance in terms of design expectations, beam-halo and synchrotron-radiation collimation efficiency.

The NLC collimation system (see Figure 1) has an additional flexibility in terms of background control – the tail folding octupoles provide an option to squeeze the beam tail distribution while not affecting the beam core. These octupoles are installed downstream of the betatron and the energy collimation system, at the very entrance to the final focus.

At the time of the TRC, the tail-folding octupoles were included only in the NLC design, so their performance was not studied in detail by the collimation task force and they were not included in the three system comparative study [2, 3]. However, in the TRC report it was noted that the wakefields for all the collimation designs would be a significant limitation – see Table 7.17 in [1]. The tail-folding octupoles can reduce the wakefields by permitting larger collimator gaps. In this paper, the performance of the NLC collimation system with octupoles will be described.

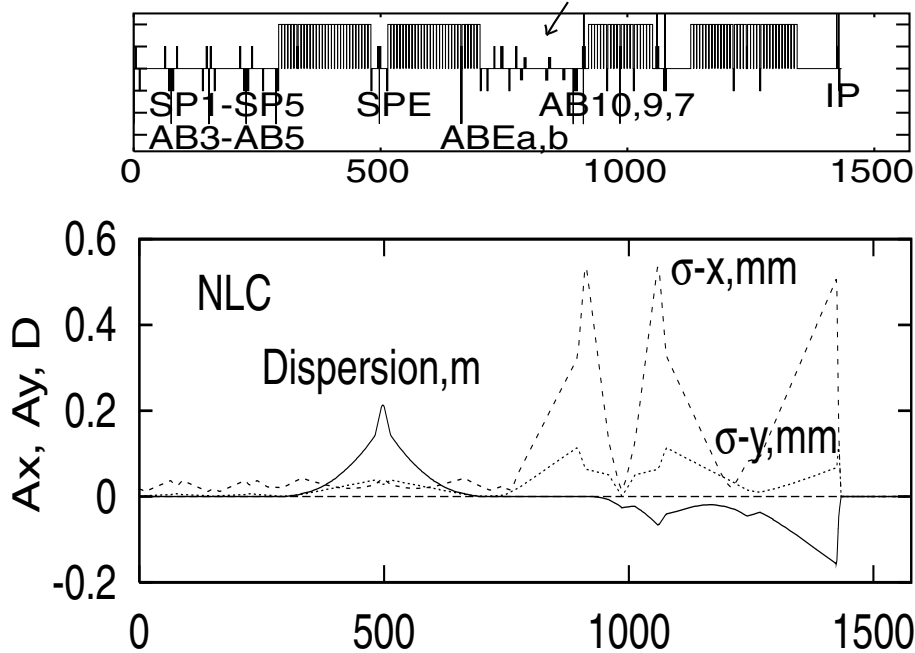


Figure 1: Optics and locations of collimators in the NLC Beam Delivery System. The location of two octupole doublets is shown by an arrow.

2 Octupole Doublets in the NLC Beam Delivery System

Nonlinear elements, such as octupoles, can in principle be used for control of the beam tails, without affecting the beam core. In practice, however, their efficiency is often limited by the difficulty of controlling all planes, see e.g. [4, 5].

A unique feature of linear colliders facilitates the use of octupoles for collimation. This is the fact that the Final Doublet (FD) phase has much more stringent collimation requirements than the Interaction Point (IP) phase. Thus, it would be sufficient for the octupoles to fold the halo only in the FD phase.

The use of octupoles for non-linear control of beam tails in the linear collider has been investigated for the linac [6] and for the Final Focus [7, 8]. These studies were limited to conceptual considerations only, because they were applied to a traditional Final Focus where non-local chromaticity correction resulted in large aberrations in the beam tails. Such distortions would mask any possible benefit from the octupoles. The advantages of nonlinear collimation only became evident with the new Final Focus design with local chromaticity correction which has good control of high order aberrations [9].

In order to control the beam tails in both horizontal and vertical directions simultaneously, a concept of octupole doublets was suggested in [10] and independently in [11]. The doublets provide tail focusing in both planes in a manner similar to strong focusing with quadrupoles. This concept was implemented in the latest design for the NLC Beam Delivery System [12], with two octupole doublets included to provide, ideally, a factor of four reduction of the size of the beam tails in the final doublet. More details on this can be found in [13].

The octupole tail folding is illustrated in Figure 2 which shows an idealized case of tail folding

with one or two octupoles doublets (OD), where the OD kick was modeled as x^5 , in contrast to the x^3 kick of a pure octupole which is canceled in the doublet to achieve azimuthal focusing symmetry. Figure 3 shows the actual beam phase space as tracked in a Beam Delivery with two octupole doublets. One of the important things to mention is that the strength of the octupoles and the size of the incoming halo, i.e. the collimation depth, must match.

The optics of the NLC BDS with the octupole doublet location is shown in Figure 1. The ODs are placed just at the beginning of the Final Focus, downstream of the energy collimation section. One additional octupole is placed near ODs to further improve the higher order performance.

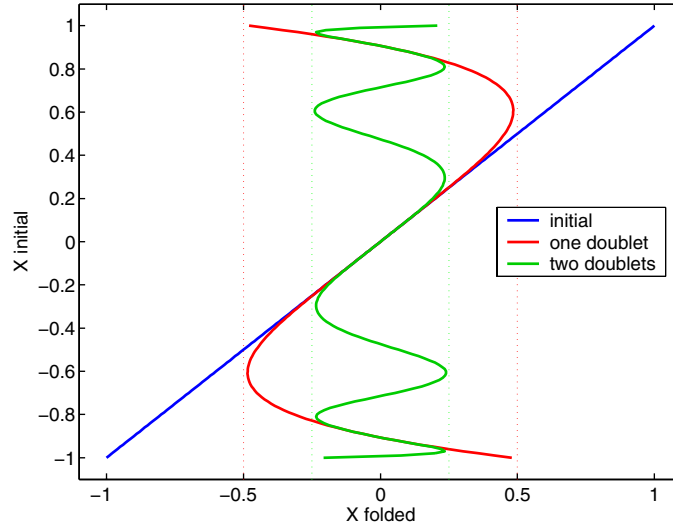


Figure 2: Illustration for tail folding octupoles showing the ideal transformation of the initial distribution of particles by an octupole-doublet-like x^5 force for one or two octupole doublets.

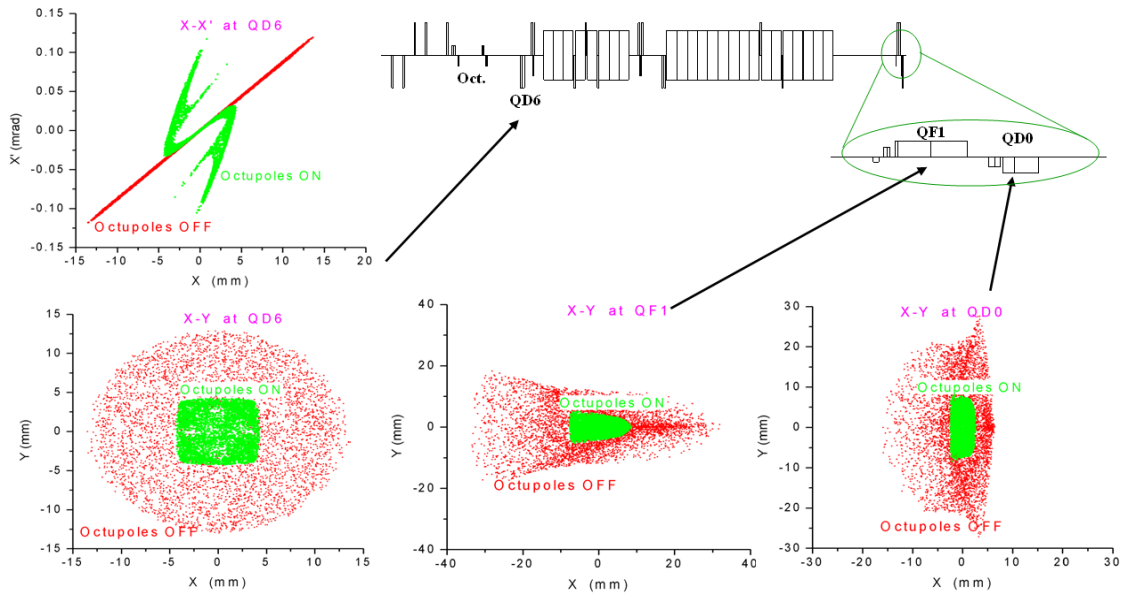


Figure 3: Illustration for tail folding octupoles in the NLC BDS. The phase space of the beam halo is shown just after the octupole doublets and in the middle of the QF1 and QD0 quadrupoles of the FD.

3 Design without Tail Folding Octupoles: Dependence on the Vertex Tilt and Radius

Before discussing results with tail folding octupoles, it is worth reconsidering the situation without octupoles. The collimator gap settings for this case are shown in Table 1.

The NLC vertex detector has a nominal internal radius of 10 mm and the length of this central detector is ± 31 mm. With a half crossing angle of 10 mrad, the vertex detector is tilted with respect to the beam direction by the same angle and this effectively reduces the horizontal aperture by 0.62 mm total (or 3%). The studies presented in [2] did not include the effects of this tilt.

Table 2 shows the synchrotron radiation and particle losses for different configurations. Case A is similar to the the configuration studied in [2] (except that the photon mask DUMP1 was offset in X). There are no losses on IR elements in this case. Case B has the vertex detector tilted by 10 mrad. One can see that photons now start to touch the vertex detector. In order to eliminate these losses, the gaps of the betatron collimators in the FD phase (SP2 and SP4) must be reduced by about 3%.

Case C in Table 2 corresponds to a vertex detector with increased aperture. The radius chosen is 11.8 mm, which is matched to the natural divergence of the synchrotron radiation fan in the IR region, discussed further below. With this radius, the losses on the vertex detector are eliminated.

S	Name	spoilers, absorbers			half-aperture			
		BetaX	BetaY	Dispers.	A_x	A_y	A_x	A_y
m		m	m	m	mm	mm	σ_x	σ_y
0.007	SP1	35.83	7.07	0.000	0.30	0.25	18.5	326
76.491	SP2	103.28	523.42	0.000	0.28	0.20	10.2	31
152.374	AB3	35.82	7.08	0.000	1.00	1.00	61.5	1304
152.491	SP3	35.82	7.08	0.000	0.30	0.25	18.5	326
228.374	AB4	103.28	523.42	0.000	1.00	1.00	36.3	153
228.491	SP4	103.28	523.42	0.000	0.28	0.20	10.2	31
288.866	AB5	59.74	5.36	0.000	1.40	1.00	66.8	1500
288.983	SP5	59.74	5.36	0.000	0.42	0.25	20.0	375
497.592	SPE	226.69	10058.96	0.213	3.20	3.20	78.3	112
662.449	ABEa	244.35	329.16	0.007	1.10	1.10	25.9	212
664.749	ABEb	240.00	283.52	0.006	1.10	1.10	26.2	228
890.421	AB10	13276.75	149854.87	0.000	4.40	4.40	14.1	40
911.000	AB9	38123.55	55295.79	0.000	6.50	3.00	12.3	45
984.952	AB7	36.63	82.44	-0.026	3.90	1.00	238	385
1363.505	DUMP0							
1384.005	DUMP1	21712.01	30406.34	-0.115	8.00	20.00	20	400
1420.795	DUMP2	33628.04	52550.49	-0.115	8.50	20.00	17.1	303
1422.955	DUMP3							
1433.815	IP							

Table 1: Horizontal and vertical β -functions, dispersion and apertures at the spoilers and absorbers in NLC without tail folding octupoles. The photon masks DUMP0 and DUMP3 were added for the octupole ON case.

The increased vertex detector radius, in fact, allows the betatron collimators located in phase with the FD (spoilers SP2 and SP4) to be opened by 25%, to 0.5 mm vertical aperture (full), which is shown in case D. In this last case, there were 75 primary particles lost in the AB7 absorber. This is at the limit of the statistical accuracy of the estimation of primary particle loss, and can be eliminated by a tiny adjustment of the AB7 gap.

Tail folding octupoles are OFF					
# bunches /(effective train)	192				
Case	A	B	C	D	C
	From halo				From core
Spoiler SP2, SP4 aperture ($X, mm \times Y, mm$)	0.56×0.40	0.56×0.40	0.56×0.40	0.56×0.50	0.56×0.40
Losses on SR mask upstream of FD					
Mean photon energy (MeV)	0.031	0.031	0.031	0.032	0.032
# photons/bunch	$3.44 \cdot 10^5$	$3.44 \cdot 10^5$	$3.44 \cdot 10^5$	$4.31 \cdot 10^5$	$7.21 \cdot 10^8$
/eff. train	$6.60 \cdot 10^7$	$6.60 \cdot 10^7$	$6.60 \cdot 10^7$	$8.28 \cdot 10^7$	$1.38 \cdot 10^{11}$
Total photon energy (GeV)					
/bunch	10.8	10.8	10.8	13.9	$2.26 \cdot 10^4$
/eff. train	2074	2074	2074	2669	$4.34 \cdot 10^6$
Losses on upstream detector mask					
QD0 radius (mm)	10	10	10	10	10
Photon Loss (mW)	0	0	0	0	0
Photon Loss (GeV/bunch)	0	0	0	0	0
Losses on vertex detector					
Radius (mm)	10	10	11.8	11.8	11.8
Vertex det. angle (mrad)	0	10	10	10	10
Photon Loss (mW)	0	$2.9 \cdot 10^{-5}$	0	0	0
Photon Loss (GeV/bunch)	0	$7.9 \cdot 10^{-3}$	0	0	0
Losses on downstream detector mask					
Lum.monitor radius (mm)	13	13	13	13	13
Photon Loss (mW)	0	0	0	0	0
Photon Loss (GeV/bunch)	0	0	0	0	0
Charged halo particle loss (part./bunch)					
SR mask	(none)	(none)	(none)	(none)	(none)
Upstream detector mask	(none)	(none)	(none)	(none)	(none)
Vertex detector	(none)	(none)	(none)	(none)	(none)
Downstream detector mask	(none)	(none)	(none)	(none)	(none)
Number of primary halo particles interacting with absorbers (part./bunch)					
	(none)	(none)	(none)	75 at AB7	(none)

Table 2: Synchrotron radiation from beam halo and core hitting IR SR mask (DUMP2), upstream detector mask, vertex detector and downstream detector mask in NLC for the case with tail folding octupoles OFF. There are no DUMP0 and DUMP3 because they are used only for the octupole ON case. These calculations were done with DUMP1 displaced by +0.5 mm in the horizontal plane (optimal displacement). The 75 particles lost on AB7 in case D is at the limit of the statistical resolution (see text).

4 Natural Apertures in the Interaction Region

The beam halo entering the final doublet naturally has some divergence which is then focused by the FD. Therefore, synchrotron radiation photons emitted in the FD would be divergent as well. This is illustrated by the Figure 4 and 5. These particular pictures were obtained with tail folding octupoles, but the results without the octupoles are similar¹.

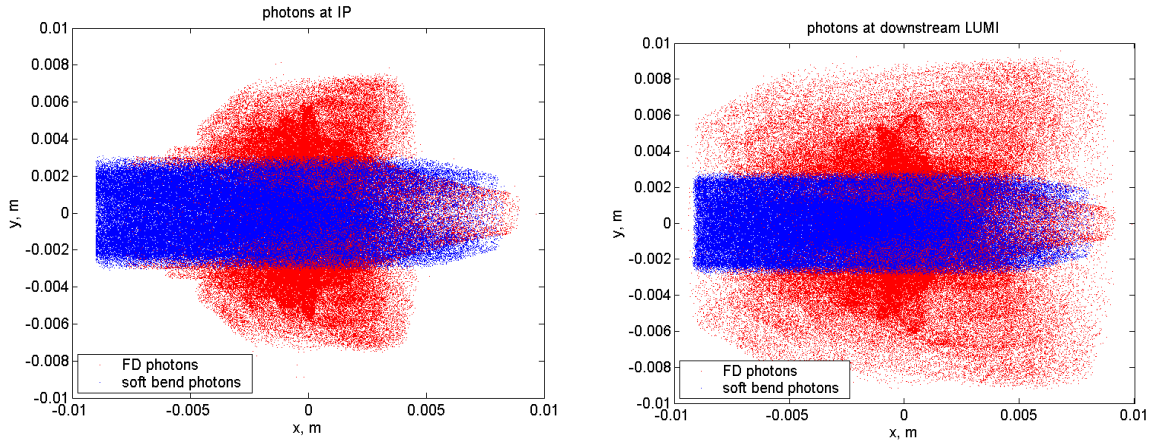


Figure 4: Photon rays at IP and at the downstream (+3.5m) luminosity monitor. The photons coming from the FD are shown in red, and the photons coming from the soft bend are shown in blue.

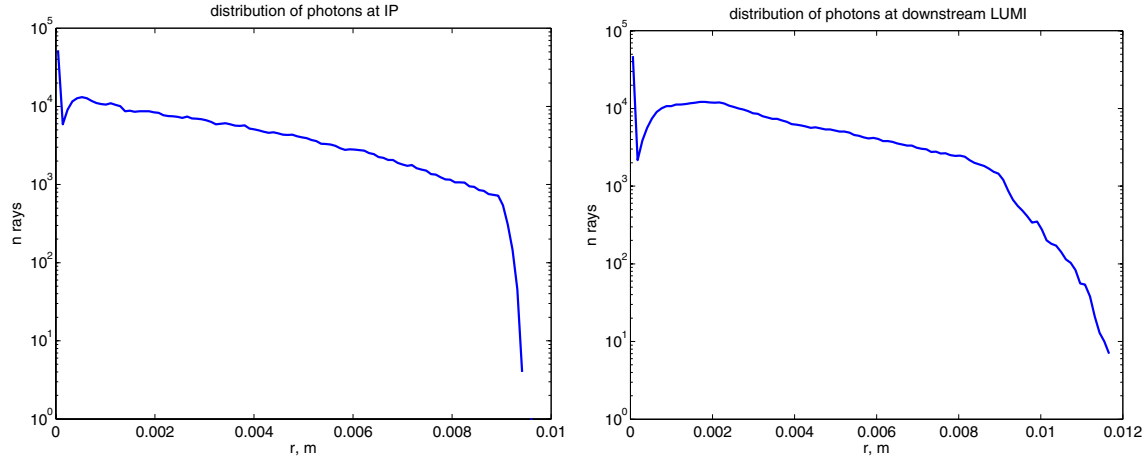


Figure 5: Distribution of photon rays versus radius at the IP and at the downstream (+3.5m) luminosity monitor.

Figure 4 shows the photon rays at the IP and at the downstream (+3.5m) luminosity monitor. The soft bend photons and photons coming from the FD are shown in different colors. One can see that while the distribution of the soft bend photons is almost unchanged, the distribution of FD photons widens by about 2 mm after the 3.5 m drift.

It would be natural therefore, from the point of view of optimizing of the protection of the IR elements, to set the apertures of the FD, Vertex, and luminosity monitor so that they increase with the photon divergence, at a minimum.

¹These photon distributions were obtained using tracking by TURTLE. Tracking with GEANT and with STRUCT [14], which was the main code used in the studies presented, gave similar results.

5 Collimation Performance with Tail Folding Octupoles

We consider below two cases where the vertex detector radius is 10 mm, and where the radius is increased to 11.8 mm, roughly correspondingly to the photon divergence. To eliminate the photon losses at the IR would require:

- Vertex radius 10 mm. Two additional synchrotron photon masks (DUMP0 and DUMP3) are needed to entirely protect the IR region.
- Vertex radius 11.8 mm. At least one or possibly two additional synchrotron photon masks (DUMP3) are needed and the strength of the octupoles is 63% of nominal.

To study these two cases in more detail, the following Table 3 illustrates the optimized collimation settings.

Case	DUMP0		DUMP1		DUMP2		DUMP3		Phot. loss in IP reg.
	$X \times Y$	part.loss							
	mm^2	part./run	mm^2	part./run	mm^2	part./run	mm^2	part./run	GeV/bunch
63% of octupole strength, vertex detector radius is 11.8 mm									
Displacement of DUMP0 is $dX=1.15$ mm, DUMP1 is $dX=0.9$ mm									
E	17×24	0	17×16	0	17×10	0	17×10	0	0.000
F	-	-	17×16	0	17×10	0	17×10	0	0.000
nominal octupole strength, vertex detector radius is 10 mm									
Displacement of DUMP0 is $dX=1.15$ mm, DUMP1 is $dX=0.9$ mm									
G	14×20	0	14×14	0	15×6	0	15×6	0	0.000

Table 3: Optimized collimator settings for the case when tail folding octupoles are ON.

With the 11.8 mm radius vertex detector, both cases E and F give an acceptable solution, when both the photon losses in the IR and the halo particle losses on the photon masks are eliminated. With the 10 mm radius vertex detector, the acceptable solution is represented by the case G. The optimal position of the photon masks is offset from the beam center. Though the wakefields due to off-centered masks were not evaluated, this is not expected to be an issue. In all cases, the betatron spoilers were opened to 1.2 mm full aperture, i.e. 3 times wider than without octupoles but with the same inner radius. Theoretically, this should be a factor of 4 wider apertures and it may be possible to approach this ideal value with further optimization.

In either of the cases E, F or G, there are no halo or primary particle losses anywhere downstream of the last absorber located in the Final Focus. Behavior of the fractional particle loss along the beamline for the case G is shown in Figure 6.

A detailed summary of the photon and particle losses is given in Table 4 where two cases are compared:

- 10 mm vertex radius (case G of Table 3);
- 11.8 mm vertex radius and no octupoles (case D of Table 2).

Calculations presented in Table 4 were performed with several different models of the halo. The first model represents a nominal halo which optimally overlaps with the collimator apertures in

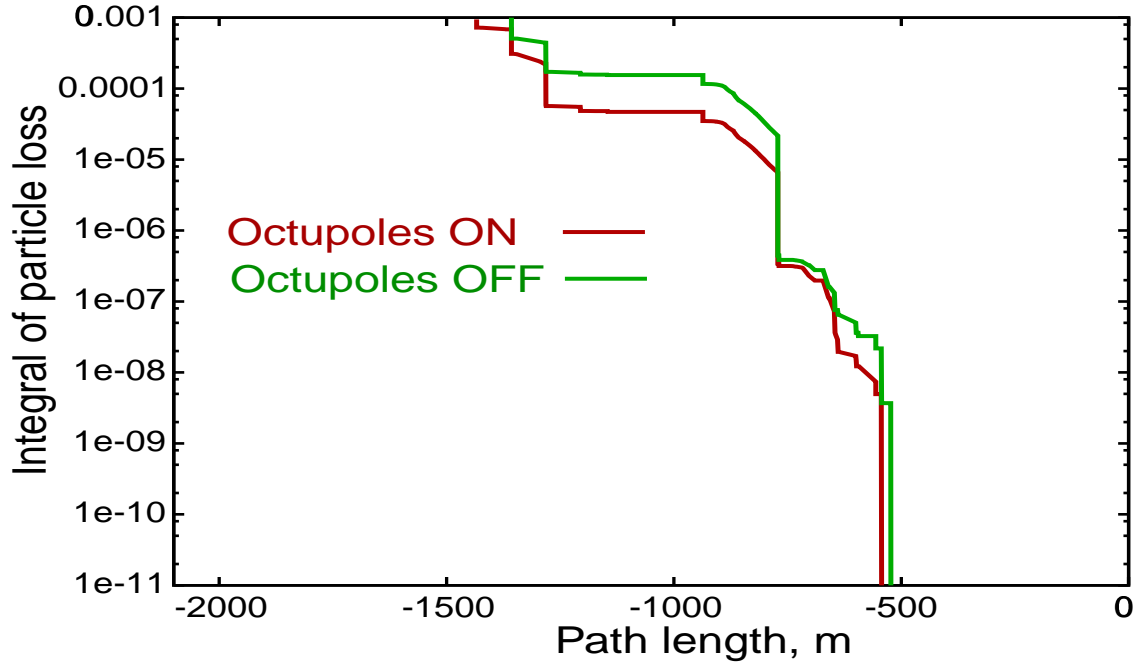


Figure 6: Fractional loss of charged-halo particles in NLC with and without tail folding octupoles.

the case without octupoles, and thus gives the most pessimistic estimation. This is the model used for studies presented in [2]. This halo model, however, would not be adequate in the case of tail folding octupoles, since the halo would not even touch the betatron spoilers which are now open wider. Therefore, a halo model which extends to a larger number of sigmas should be used to study the octupole ON case. For consistency, this larger halo model was also applied to the octupole OFF case.

From halo				
	Tail folding octupoles are OFF		Tail folding octupoles are ON	
Halo model	$6 - 16\sigma_x$ $24 - 73\sigma_y$	$6 - 200\sigma_x$ $24 - 300\sigma_y$	$10 - 200\sigma_x$ $50 - 300\sigma_y$	$6 - 200\sigma_x$ $24 - 300\sigma_y$
# bunches /(effective train)	192			
SP2, SP4 full aperture ($X, mm \times Y, mm$) ($X, \sigma_x \times Y, \sigma_y$)	0.56×0.50 $\pm 10 \times \pm 39$		1.20×1.20 $\pm 22 \times \pm 92$	
Losses on SR mask (DUMP0) upstream of FD				
Mean photon energy (MeV)	(not used)		0.789	0.587
# photons/bunch	(not used)		$2.05 \cdot 10^6$	$2.99 \cdot 10^6$
/eff. train	(not used)		$3.94 \cdot 10^8$	$5.74 \cdot 10^8$
Total photon energy (GeV)	(not used)		$1.62 \cdot 10^3$	$1.75 \cdot 10^3$
/bunch	(not used)		$3.11 \cdot 10^5$	$3.36 \cdot 10^5$
/eff. train	(not used)			
Losses on SR mask (DUMP1) upstream of FD				
Mean photon energy (MeV)	0.191	0.191	0.037	0.037
# photons/bunch	$3.77 \cdot 10^6$	$6.66 \cdot 10^5$	$2.25 \cdot 10^5$	$3.38 \cdot 10^5$
/eff. train	$7.24 \cdot 10^8$	$1.27 \cdot 10^8$	$4.32 \cdot 10^7$	$6.49 \cdot 10^7$
Total photon energy (GeV)				
/bunch	718	127	8.39	12.3
/eff. train	$1.38 \cdot 10^5$	$0.24 \cdot 10^5$	1610	2362
Losses on SR mask (DUMP2) upstream of FD				
Mean photon energy (MeV)	0.032	0.031	0.033	0.034
# photons/bunch	$5.16 \cdot 10^5$	$0.91 \cdot 10^5$	$1.57 \cdot 10^5$	$2.42 \cdot 10^5$
/eff. train	$9.91 \cdot 10^7$	$1.75 \cdot 10^7$	$3.01 \cdot 10^7$	$4.65 \cdot 10^7$
Total photon energy (GeV)				
/bunch	16.5	2.86	5.12	8.31
/eff. train	3168	549	983	16
Losses on SR mask (DUMP3) upstream of FD				
Mean photon energy (MeV)	(not used)		0.031	0.038
# photons/bunch	(not used)		$5.72 \cdot 10^3$	$8.46 \cdot 10^3$
/eff. train	(not used)		$1.10 \cdot 10^6$	$1.62 \cdot 10^6$
Total photon energy (GeV)	(not used)			
/bunch	(not used)		0.175	0.317
/eff. train	(not used)		33.6	60.7
Losses on upstream detector mask				
QD0 radius (mm)	10		10	
Photon Loss (GeV/bunch)	0		0	
Losses on vertex detector				
Radius (mm)	11.8		10	
Vertex det. angle (mrad)	10		10	
Photon Loss (GeV/bunch)	0		0	
Losses on downstream detector mask				
Lum.monitor radius (mm)	13		13	
Photon Loss (GeV/bunch)	0		0	
Charged halo particle loss (part./bunch)				
SR mask	(none)		(none)	
Upstream detector mask	(none)		(none)	
Vertex detector	(none)		(none)	
Downstream detector mask	(none)		(none)	
Number of primary halo particles interacting with absorbers (part./bunch)				
Absorbers in FF	75 at AB7		(none)	

Table 4: Synchrotron radiation from beam halo hitting IR SR masks (DUMP0, DUMP1, DUMP2, DUMP3), upstream detector mask, vertex detector and downstream detector mask, with the tail folding octupoles off and on. Calculations are done with different halo distributions for cases octupoles “off” and “on”, and with the same halo distribution for both cases. Synchrotron radiation mask positions are the same for both cases (optimized for octupoles “on”). The number of particles lost on AB7 is at the limit of statistical resolution.

6 Conclusion

The collimation performance of the NLC Beam Delivery System has been evaluated for a configuration with tail folding octupoles. With these octupoles, it is possible to find an optimal configuration of spoiler and absorber gaps and photon masks, so that there are no charged particles lost anywhere downstream of the last collimator in the Final Focus (more than 500 m from the IP), and there are no synchrotron photons lost anywhere in the Interaction Region.

With tail folding octupoles, the betatron spoilers can be opened by at least a factor of 3, to 1.2 mm full aperture, reducing the effect of collimator wakefields.

References

- [1] Second ILC-TRC Report, SLAC-R-606, 2003.
- [2] A. Drozhdin, et al., FERMILAB-TM-2200, NLC LCC-0111, SLAC, 2003.
- [3] A. Drozhdin, et al., PAC 03, Portland, Oregon, May 2003, p.2739.
- [4] P.F. Meads, IEEE Trans Nuc Sci NS30, 1983, p.2838.
- [5] N. Tsoupas, et al., PAC91, (1991), p.1695.
- [6] R. Pitthan, SLAC-PUB-8402, 1999.
- [7] F. Zimmermann, NLC Acc Phys Note, July 14 1998, <http://www-sldnt.slac.stanford.edu/nlc/notes/octfd.ps>
- [8] R. Helm, SLAC, unpublished, 1999-2000.
- [9] P. Raimondi, A. Seryi, PRL 86, 3779 (2001).
- [10] P. Raimondi, NLC MAC meeting, May 2001, SLAC, http://www-project.slac.stanford.edu/lc/local/MAC/MAY2001/Talks/Mac_May%20Panta.pdf
- [11] R. Brinkmann, BDIR2000 workshop, July 2000.
- [12] 2001 Report on the Next Linear Collider (“Copper Book” – a Report Submitted to Snowmass 2001), SLAC-R-571, June 2001.
- [13] R. Brinkmann (DESY), P. Raimondi, A. Seryi (SLAC), “Halo Reduction by Means of Non Linear Optical Elements in the NLC Final Focus System”, in Proceedings of PAC2001, June 2001.
- [14] I. Baishev, A. Drozhdin, and N. Mokhov, ‘STRUCT Program User’s Reference Manual’, SSCL-MAN-0034 (1994), <http://www-ap.fnal.gov/~drozhdin/>